Structural properties of some defects in tin-dioxide (SnO_2)

JN Ntimane, TE Mosuang[1], KE Rammutla[1]

1. Department of Physics and Geology, University of Limpopo, Private Bag X 1106, Sovenga, 0727, Polokwane, South Africa

thuto.mosuang@ul.ac.za

Abstract. Tin-dioxide ceramics have been intensively studied in recent years because of the potential in sensing and fuel cells. The present work uses classical molecular dynamics simulations focused on the role of defects in tin-dioxide. The total energy of the NPT hoover ensemble at various temperatures has been calculate in order to determine the effects of oxygen vacancy and Ti substitutional defect in tin-dioxide. The results obtained showed an energy increase with temperature which was constantly compared with experiments. The radial distribution functions for the structures suggest the transformation of anatase to rutile tin-dioxide at high temperature.

1. Introduction

Structural and thermodynamic properties of metal-oxide materials like tin oxide (SnO_2) play crucial role as semiconducting sensors and electronic devices. The manifestation of intrinsic bulk and surface defect levels and the origin of extrinsic defect levels are of practical significance in the functioning property of these materials. The well-known reflectivity and conductivity property of SnO_2 are influenced by intrinsic native defects. In general, SnO_2 defects show up as oxygen vacancies. These introduce energy levels into the energy gap of the material causing the n-type conduction of states filled near the conduction band minimum. For effective use as sensors and semiconductors, these materials must have good transmittance of the visible light and resistivity well below 10^{-3} Ωcm.

A great deal of experimental investigation has been performed on various forms of SnO_2 including the current nanoscale studies. Jones *et al* performed some scanning tunnelling microscopy measurements on the surface structure whilst Cox *et al* performed ion-scattering spectroscopy together with ultraviolet photoelectron measurements on the surface of SnO_2 to understand the oxygen vacancy defect in the conductivity of SnO_2. Now advanced computer softwares based on empirical and first principle calculations make it possible to study the bulk, surface, and nanostructures of this material. Such development permits formation of an atomistic image of semiconduction and sensing mechanisms. Noteworthy, the first principle calculations are limited to zero temperature, although high temperature environments are responsible for a number of kinetic factors observed in thin films, surfaces, and nanoparticles. Subsequently, metal oxide sensors work at elevated temperatures, which also influence the impurity adsorption and catalytic processes in the material matrix. Through the molecular dynamics approach for the defects in SnO_2, simulations at high temperatures can be achieved with ease.

The aim of this paper is to highlight some notable structural and thermodynamic properties obtained when anatase SnO_2 is subjected to oxygen vacancy defect and titanium substitutional defect. The empirical molecular dynamics using the Buckingham potentials has been used through the

simulations. Hopefully these results will provide an atomistic understanding of the role of defects in semiconducting sensors.

2. Computational details

Empirical molecular dynamics (MD) has been used to model the anatase SnO_2 and the related defects.A tetragonal space group $I4_1/amd$ SnO_2 unit cell has been repeated periodically in 3 dimensions to make a supercell with 192 Sn atoms and 384 O atoms. The oxygen parameter for anatase is 0.2066 Å and there are four Sn-O distance of 1.937 Å and two of 1.964 Å [7]. In the case of an oxygen vacancy defect on oxygen atom has been removed to make 383 O atoms. A Sn atom has also been replaced by a Ti atom in order for a substitutional Ti defect to materialize.

The material was modelled using the Buckingham potentials [8]. The DL-POLY package [8] has been used to perform all the empirical bond-order molecular dynamics calculations of SnO_2. A supercell with a 7.29 cutoff, 576 atoms, and a sufficiently larger number grid points for the fast Fourier transformations(kmax1=6,kmax2=6, and kmax3=12) has been used for anatase SnO_2 throughout the calculations. The ewald convergence parameter of 0.3975 for anatase, on a Noose-Hoover NPT ensemble allowing the simulation supercell to change has been applied. The thermostat relaxation was set at 0.1 whilst the barostat was at 0.5. The simulation was allowed to run for more than 100 000 steps, with a simulation time step of 0.001ps.The controlled experimental crystal structure for anatase SnO2 is according to Cromer and Herrington [7]. The material as is used for the molecular dynamics(MD) modeling is described by its lattice parameters as listed in Table 1, and a set of parameters required for the Buckingham potential are taken from AV Bandura *et al.* [9] and P Amstrong *et al*. [10]. Energy parameters were determined so as to reproduce the observed crystallographic structures of anatase SnO_2 and the accompanying dopants.

Table 1. The lattice parameters and relative sites for O atom and Sn-O bonds [7].

	this work	experiments
a (Å)	3.8263	3.7845
b (Å)	11.3194	9.5143
u	0.208	0.2066
Sn-O (Å)	4 x 2.1, 2 x 2.0	4 x 1.937, 2 x 1.964

3. Results and discussion

In Table I, the simulated lattice parameters of anatase SnO_2 are shown. The results show that the two-body Buckingham potential reproduce the crystallographic structures within the experimental results.

In this paper the thermodynamic properties of anatase SnO_2 together with oxygen vacancy defect (V_O) in anatase SnO_2 and a Ti subsititutional defect Ti_{Sn} in anatase SnO_2 are being explored. The calculations have been performed above SnO_2 Debye temperature of 570 K by Tuerkes *et al*. [11] and 620 K by Bachmann *et al.* [12]. Subsequently the MD treats the motion of atoms classically; above the Debye temperature quantum mechanical effects can be neglected. So the average of the two, Debye temperatures was estimated at 595 K. Figure 1 shows the volume of anatase SnO_2, V_O, and Ti_{Sn} as functions of temperature above the SnO_2 Debye temperature. From the plots it can be seen that Ti_{Sn} curve has the lowest volume throughout the temperatures. This suggests that the presence of Ti substitutional defect in SnO_2 could assist in reduction of grain growth as argued by Rumyantseva *et al.* [13]. The volume thermal expansion coefficient for anatase SnO_2 was calculated to be 8.08×10^{-6} K^{-1}, of which differs by a few orders from the measured valued of 11.7×10^{-6} K^{-1} by Peercy and Morosin [14]. Of course it should also be noted that Peercy and Morosin Raman measurements were done on a rutile SnO_2 structure.

The specific heat of anatase SnO_2 has also been calculated with the increasing volume. This is obtained from the temperature derivative of the total energy of the system. Figure 2 shows the said plot of energy against temperature for anatase SnO_2, oxygen vacancy V_O, substitutional Ti_{Sn}. The

specific heat calculated is $3.41k_B$ which differ by about 12% from the Dulong-Petit's law of solids at high temperatures. But even the measured values seem to be more offline with the value $6.32k_B$ [15]. It can be seen on the plots that substitutional Ti_{Sn} has the lowest energy, which suggest a good dopant for enhanced conductivity. Likewise, the oxygen vacancy V_O and the anatase SnO_2 curve intersect around 3000 K, which suggest an anticipated high temperature transition to the rutile SnO_2 phase in agreement with the Fan and Reid [16] measurements.

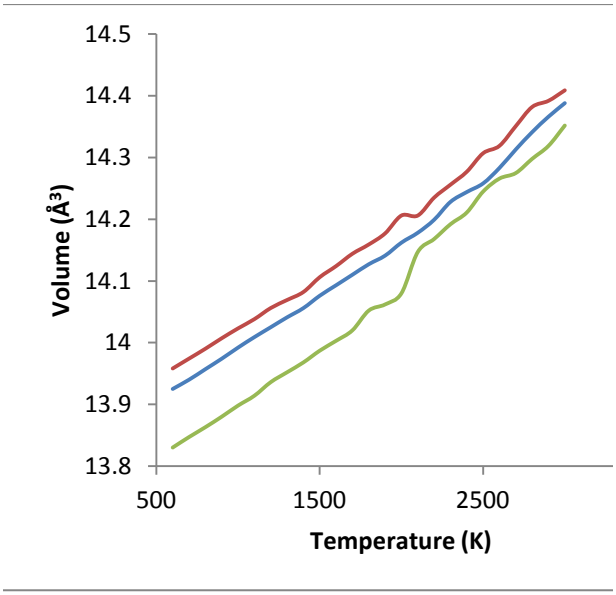

Figure 1. Volume as function of temperature for anatase SnO_2. blue curve is anatase SnO_2, red curve is V_O, and green curve is Ti_{Sn}.

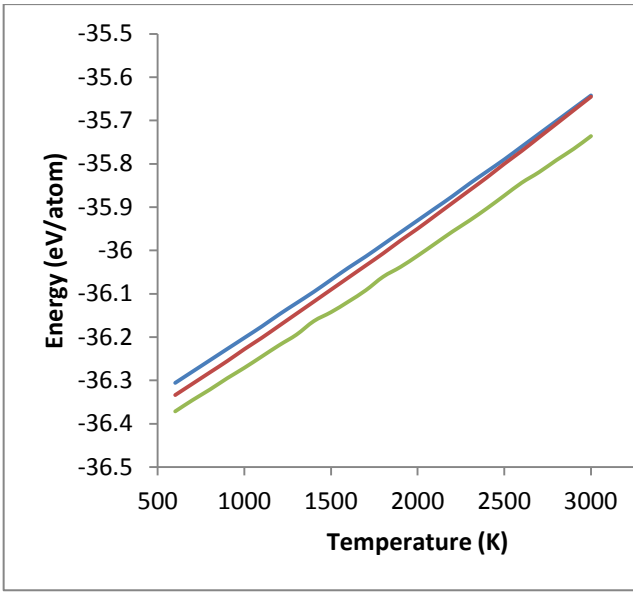

Figure 2. Energy as function of temperature for anatase SnO_2. blue curve is anatase SnO_2, red curve is V_O, and green curve is Ti_{Sn}.

In order to further check the stability of anatase SnO_2 and its two defects at various temperatures within the Buckingham potential, the radial distribution functions of SnO_2 at 300 K and 5000 K are presented in Figure 3 and 4. The peaks show the most probable distances between the atoms concerned. Furthermore, Figure 4 shows that at 5000 K, the peak positions for anatase SnO_2 look the same as that of the rutile SnO_2 at 300 K to 1000 K, with notable peak shifts in the rutile SnO_2 [17]. The same form of peak positions is experienced with the substitutional Ti_{Sn}. This suggest a probable phase transition from anatase to rutile SnO_2 in agreement with the first principle calculations of Yanlu Li *et al.* [18] and the experiments of Bachmann et al. [12] and Fan and Reid [16]. On the other hand these calculations show stability and transferability of the Buckingham potentials in structural analysis of materials.

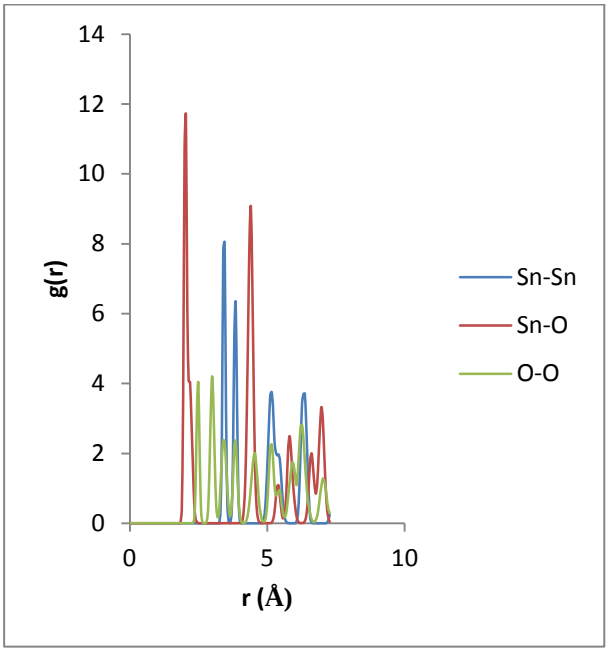

Figure 3. Radial distribution function of anatase SnO_2 at 300 K.

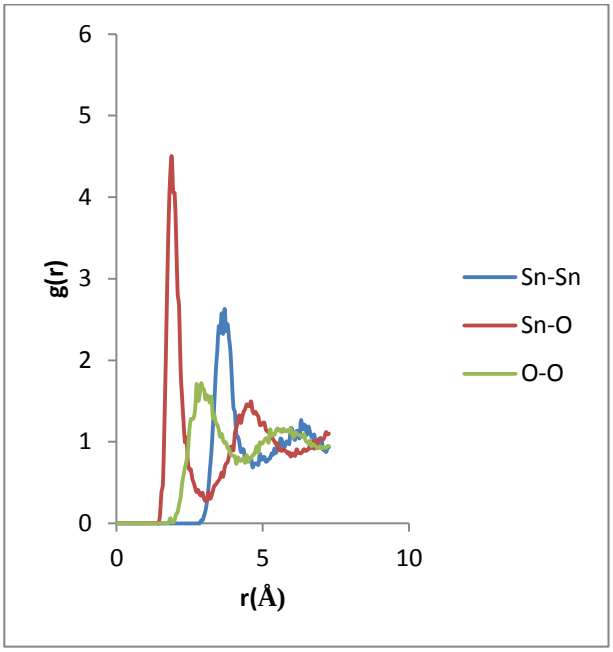

Figure 4. Radial distribution function of anatase SnO_2 at 5000 K.

4.Conclusion

Anatase SnO_2, oxygen vacancy in SnO_2 and Ti substitutional defect in SnO_2 have been modelled with molecular dynamics simulation using the Buckingham potential to investigate their structural and thermodynamic properties. The radial distribution curves and the energy-temperature graph suggest phase transformation at temperatures around 3000 K. Ti substitutional defect in anatase SnO_2 has the lowest energy and lowest volume which could improve its semiconducting properties at a controlled nanocrystalline growth. The volume thermal expansion coefficient is of the same order as the measured results. The specific heat capacity is of the same order with the Dulong-Petit law of solids at high temperatures.

5.Acknowledgements

IBSA, NRF and UL are thanked for their financial support. CHPC is thanked for their computational facilities.

References

[1] Godinho KG, Walsh A and Watson GW 2009 *J. Phys. Chem.* C **113** 439
[2] Lantto V, Rantala TT and Rantala TS 2001 *Journal of the European Ceramic Society* **21** 1961
[3] Jones FH, Dixon R, Foord JS, Edgell RG and Pethica JB 1997 *Surface Science* **376** 367
[4] Cox DF, Fryberger TB and Semancik S 1988 *Phys. Rev. B* **38** 2072
[5] Freeman CM and Catlow CRA 1990 *J. Solid State Chem.* **85** 65
[6] Hines RI, Allan NL and Flavell WR 1996 *J. Chem. Soc., Faraday Trans.* **92** 2057
[7] Cromer DT and Herrington K 1955 *Contribution from the national Lead Co., Titanium division* **77** 4708
[8] Smith W, Forester TR and Todorov IT 2009 *DL_POLY_2 User Manual*, STFC Daresbury Laboratory, Daresbury, Warrington WA4 4AD, Cheshire, UK

[9] Bandura AV, Sofo JO and Kubicki JD 2006 *Journal of Chemistry* B **110** 8386

[10] Amstrong P, Knieke PC, Mackovic M, Frank G, Hartmaier A, Goken M and Peukert W 2003 *Acta Materialia* **57** 3060
[11] Tuerkes P, Pluntke Ch and Morosin D 1973 *Journal of Physics* C **13** 4941
[12] Bachmann KJ, Hsu FSL and Remeika JP 1981 *Physica Status Solidi* (a) **67** K39
[13] Rumyantseva MN, Sefonova OV, Boulova MN, Ryabova LI and Gas'kov AM 2003 *Russian Chemical Bulletin* **52** 1217
[14] Peercy PS and Morosin D *1973 Physical Review* B **7** 2779
[15] D'Ans-Lax:Taschenbuch f. Chemiker u. Physiker, Vol 1, Berlin, Heidelburg, New York: Spring 1967
[16] Fan H and Reid SA 2003 *Chemistry of Materials* **15** 564
[17] Ntimane JN, Mosuang TE and KE Rammutla 2011 *Proceedings of the SAIP2011* 268
[18] Li Y, Fan W, Sun H, Cheng X, Li P, Zhao X, Hao J and Jiang M 2010 *J. Phys. Chem.* A 114 1052